Metal–Organic Framework (MOF) as a Precursor for Synthesis of Platinum Supporting Zinc Oxide Nanoparticles

Bo Liu,[1,2] Song Han,[1] Koji Tanaka,[1] Hiroshi Shioyama,[1] and Qiang Xu*[1,2]

[1]National Institute of Advanced Industrial Science and Technology (AIST), Ikeda, Osaka 563-8577

[2]Graduate School of Engineering, Kobe University, Nada-ku, Kobe 657-8501

Received February 18, 2009; E-mail: q.xu@aist.go.jp

Nanocrystalline ZnO-supported platinum nanoparticles were synthesized by introducing inorganic platinum salt into the pores of MOF-5 ($[Zn_4O(bdc)]_3$; bdc = 1,4-benzenedicarboxylate) followed by heating in air at 600 °C. The Pt particle sizes can be controlled by adjusting Pt precursor concentration. The resultant Pt/ZnO samples displayed higher catalytic activity for CO oxidation than conventional Pt/ZnO catalyst.

Metal–organic frameworks (MOFs) have shown rapid growth during the past decade, benefitted from the successful application of secondary building units (SBUs), and exhibit potential applications in many fields including hydrogen storage, and catalysis.[1] Generally, MOFs show two features: one is SBUs and the other is versatile pore structures and topologies. Currently, more interest has been focused on the control and application of the pores in MOFs,[1] while little attention has been placed on the application of the SBUs. SBUs are generally built up with metal and coordinated atoms (for instance, N, O, and S) in the way of metal oxide (nitride and sulfide) subunits. In a previous work, we introduced small organic molecules into the pores of MOF-5 ($[Zn_4O(bdc)_3]$, bdc = 1,4-benzenedicarboxylate)[1h] followed by polymerization and carbonization to synthesize nanoporous carbon and found that metal oxide subunits in MOF-5 assembled into nanocrystals during treatment at high temperature.[2] On the other hand, supported metal catalysts, especially for noble metals, exhibit good catalytic activities for various reactions such as CO oxidation,[3] hydrogenation,[4] and water-gas shift.[5] Investigations have verified that the catalytic activities depend on the size, shape, and chemical nature of supports and the interaction between metals and supports, all of which are involved in the preparation process.[3] In this work, we specify a strategy for the first time to synthesize ZnO-supported platinum nanoparticles via introducing an inorganic platinum salt into the pores of MOF-5 followed by heating, taking advantage of the ZnO subunits in MOF-5. The sizes of platinum nanoparticles can be tuned by changing the concentration of platinum precursor. The prepared nano-structured Pt/ZnO samples displayed higher catalytic activity for CO oxidation than conventional Pt/ZnO catalyst.

Experimental

MOF-5 used in this work was prepared according to the literature.[6] Powder X-ray diffraction of MOF-5 was measured to verify its phase purity.

MOF-5 was pretreated under dynamic vacuum at 200 °C for 24 h to free the pores in MOF-5. The degassed MOF-5 was soaked in platinum tetrachloride DMF solution (0.1, 0.025, and 0.005 M). The mixture was placed under vacuum to make solution fully penetrate into the pores of MOF-5 for 30 min. After filtrating and washing with DMF, the residue was heated at 600 °C for 1 h in air, which leads to the formation of Pt/ZnO samples (denoted as $Pt_{0.1}$/ZnO, $Pt_{0.025}$/ZnO, and $Pt_{0.005}$/ZnO according to Pt precursor concentration).

CO catalytic oxidation was conducted using a TPR system equipped with an online mass spectrometer (MS). Mass flows of CO, O_2, and Ar were controlled by mass flow controllers (Brooks). Typically, Pt/ZnO sample ($Pt_{0.1}$/ZnO (75 mg), $Pt_{0.025}$/ZnO (300 mg), and $Pt_{0.005}$/ZnO (1500 mg)) was diluted by quartz sand (6.93 g, 30–60 mesh) and the mixture was charged into a reactor made of stainless steel. The catalyst was pretreated by heating at 350 °C for 2 h, and then cooled down to room temperature in an Ar flow. Subsequently, a gas mixture (CO 1%, O_2 21%, Ar 78%, total rate of 150 mL min^{-1}, 1 atm) was fed into the reactor. The temperature inside the reactor was monitored by a thermocouple extending into the catalyst bed. After inlet gas reached a steady state in about 3 h, the steady-state catalytic activity was measured, during which the outlet gas was detected by online MS. The CO conversion (X_{CO}) is defined as follows:

$$X_{CO} = (N_{CO,in} - N_{CO,out})/N_{CO,in} \times 100\% \quad (1)$$

where N is mol of CO. In the absence of a catalyst, there is no measurable conversion of CO in the temperature range of interest.

Results and Discussion

MOF-5,[1h] one of the most representative MOFs, contains Zn_4O_{13} built from four ZnO_4 tetrahedra sharing a common vertex and six carboxylate carbon atoms that define an octahedral SBU joined by benzene links, and has a three-dimensional intersecting channel system (cavity diameter 18 Å). Platinum tetrachloride was introduced into the pores of degassed MOF-5 by the incipient wetness method and then the mixture was washed with DMF. Subsequent heating leads to the formation of Pt/ZnO samples. During the heating process, the MOF-5 was decomposed into ZnO while platinum tetrachloride accommodated in the pores of MOF-5 was also directly decomposed to Pt, giving rise to the formation of platinum-supporting zinc oxide (Pt/ZnO) nanoparticles (Pt 5.0 wt% determined by inductively coupled plasma (ICP) spectrometry for $Pt_{0.1}$/ZnO sample) as schemed in Figure 1. Undoped ZnO nanocrystals were prepared by directly heating MOF-5 at 600 °C for 1 h in air.

FTIR spectra (Figure 2) were recorded at room temperature to verify the stability of Zn–O subunits in MOF-5 samples heated at temperatures ranging from 100 to 600 °C. The commercial ZnO (Alfa) was also measured for comparison. For the MOF-5 samples heated from 100 to 400 °C, the absorption peak centered at about 520 cm^{-1} is attributed to the vibration of

Published on the web August 7, 2009; doi:10.1246/bcsj.82.1052

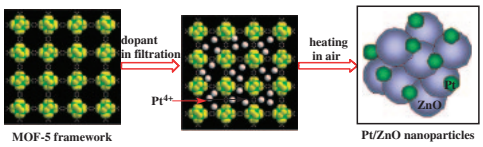

Figure 1. Growth illustration of Pt/ZnO nanoparticles.

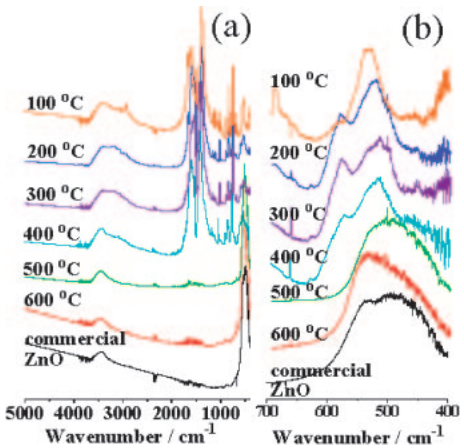

Figure 2. FTIR spectra of MOF-5 treated at different temperatures as well as commercial ZnO in the ranges of (a) 5000–400 and (b) 700–400 cm^{-1} (the enlarged region of (a)).

Zn–O in MOF-5.[7] With the temperature increasing to 500 and 600 °C, all the peaks from MOF-5 disappear except the band for Zn–O, agreeing well with that of the commercial ZnO. The formation mechanism of ZnO nanocrystals in the present work is much different from the metal–organic chemical vapor deposition (MOCVD) method, where the zinc originates from the decomposition of organozinc compounds and additional oxidants such as O_2 and N_2O are necessary.[8] In contrast, the intrinsic Zn–O subunits in MOF-5 as a ZnO source were directly assembled into the ZnO nanocrystals in our method.

Powder XRD patterns were measured to examine the crystal structures of the ZnO and Pt/ZnO samples (Figure 3a). The diffraction peaks match well with the wurtzite structural ZnO (JCPDS 36-1451) and platinum (JCPDS 04-0802). For the $Pt_{0.025}$/ZnO and $Pt_{0.005}$/ZnO samples, the signals of Pt are weak because of the low Pt contents. More structural details were investigated by TEM (Figure 3), where the sizes of Pt particles decrease with the decreasing Pt precursor concentration, ranging from 10 ($Pt_{0.1}$/ZnO) and 5 ($Pt_{0.025}$/ZnO) to 2 nm ($Pt_{0.005}$/ZnO), while ZnO particles with average diameters of 30 nm are observed for all three samples. When only MOF-5 was heated under the same conditions, ZnO nanocrystals were formed with a similar diameter (30 nm). We can conclude that the size of ZnO particles is determined by the MOF employed, regardless of the Pt precursor concentration and the sizes of Pt particles can be controlled by adjusting the Pt precursor concentration. The X-ray diffraction peaks and the lattice fringes observed from high-resolution TEM (HRTEM) for $Pt_{0.1}$/ZnO (Figure 3g) demonstrate that ZnO and Pt nanoparticles are highly crystalline. The X-ray photoelectron energy spectrum (XPS) of $Pt_{0.1}$/ZnO samples for the binding energy of the Pt (4f) core level region (Figure 4) indicates two peaks

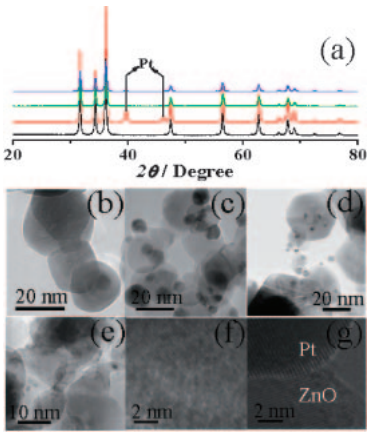

Figure 3. (a) Powder X-ray patterns of as-prepared ZnO (black line), $Pt_{0.1}$/ZnO (red line), $Pt_{0.025}$/ZnO (green line), and $Pt_{0.005}$/ZnO (blue line); TEM images of as-prepared (b) ZnO, (c) $Pt_{0.1}$/ZnO, (d) $Pt_{0.025}$/ZnO, and (e) $Pt_{0.005}$/ZnO; HRTEM images of as-prepared (f) ZnO and (g) $Pt_{0.1}$/ZnO.

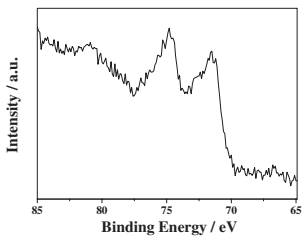

Figure 4. XPS of Pt (4f) core level region for the as-prepared $Pt_{0.1}$/ZnO sample.

centered at 74.8 and 71.5 eV, corresponding to the metallic Pt species, which agrees well with the XRD result.

An advantage of the MOF route is the facile introduction of metal precursors into the pores leading to supported metal particles of uniform size resulting from the intrinsic metal oxide subunits and pores of the MOF. Interestingly, this approach makes feasible preparation of nano-sized metal oxide support, deriving from assemble of the metal oxide subunits in MOFs in one step, which is difficult to accomplish by the conventional wet techniques with bulk metal oxides as supports. Importantly, the sizes of the noble metal nanoparticles can be controlled, which is vital for practical applications.

Various supported platinum catalysts have been documented for catalytic CO oxidation[3a,3c,3e] and different mechanisms of CO oxidation have been proposed.[9] In the present work, CO oxidation by O_2 was performed over the prepared Pt/ZnO samples using a temperature-programmed reaction (TPR) instrument equipped with a quadrupole mass spectrometer (MS). The percentage of CO conversion as a function of temperature is presented in Figure 5. Complete CO conversions were reached at 154 and 160 °C for $Pt_{0.1}$/ZnO and $Pt_{0.025}$/ZnO, respectively. The catalytic activity is enhanced when the diameter of Pt particle is reduced to 2 nm ($Pt_{0.005}$/ZnO), for which complete conversion was reached at lower temperature (140 °C). It has been reported that 100% CO conversion can be achieved at a temperature of 160 °C over Pt/ZnO composite prepared by colloidal approach[10] and that Pt/γ-Al_2O_3 and Pt/TiO_2 pretreated at varied conditions gives rise to the 100% CO

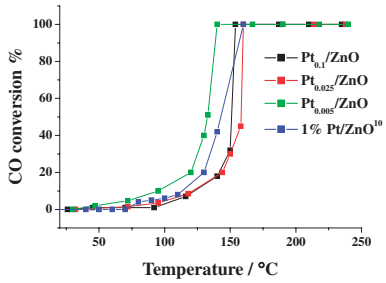

Figure 5. Conversion of carbon monoxide ($CO:O_2:Ar = 1:21:78$, total flow rate, 150 mL min^{-1}; 1 atm) over the $Pt_{0.1}/ZnO$ (75 mg), $Pt_{0.025}/ZnO$ (300 mg), and $Pt_{0.005}/ZnO$ (1500 mg) catalysts as a function of temperature. The Pt contents were normalized to the same for the three catalysts. The catalytic activity data of 1% Pt/ZnO was taken from Ref. 10 for comparison.

Table 1. Comparison of Reaction Conditions and Catalytic Activities for CO Oxidation over Various Catalysts

	Catalysts			
	$Pt_{0.1}/ZnO$	Pt/ZnO[10]	Pt/Al_2O_3[3e]	Pt/TiO_2[3e]
Preparation method	MOF route	Colloid deposition route	Incipient wetness impregnation	Incipient wetness impregnation
Pretreatment conditions	350 °C, 2 h, Ar flow	300 °C, 4 h, O_2/Ar flow	400 °C, H_2 flow	200 °C, H_2 flow
$CO:O_2$:balance gas	1:21:78	0.5:10:89.5	1:21:78	1:21:78
GHSV /mL g^{-1} h^{-1}	120000	120000	120000	120000
$T_{\text{conversion 100\%}}$ /°C	154	160	240	200

conversion at temperatures above 240 °C and around 200 °C, respectively.[3e] The detailed comparison of reaction conditions and catalytic activities over various catalysts are summarized in Table 1. The surface areas (S) have been theoretically calculated by taking the diameters of platinum particles and ZnO as observed by TEM for $Pt_{0.1}/ZnO$ ($S = 27.96\ m^2\ g^{-1}$, $d = 10$ nm), $Pt_{0.025}/ZnO$ ($S = 55.92\ m^2\ g^{-1}$, $d = 5$ nm), $Pt_{0.005}/ZnO$ ($S = 139.79\ m^2\ g^{-1}$, $d = 2$ nm), and ZnO ($S = 35.68\ m^2\ g^{-1}$, $d = 30$ nm) ($S = 6/d\rho$, d: particle diameter; ρ: density, 21460 and 5606 kg m^{-3} for platinum and zinc oxide, respectively). Turnover frequencies (TOF) are calculated to be 0.53 and 0.27 s^{-1} at 160 °C for $Pt_{0.1}/ZnO$ (radius of Pt particles, 5 nm; CO flow rate, 1.5 mL min^{-1}) and Pt/ZnO (1%) prepared by colloidal deposition (radius of Pt particles, 1 nm; CO flow rate, 0.5 mL min^{-1}),[10] respectively. The surface density (ρs) of platinum atoms is taken as 1.25×10^{19} atoms per square meter.[11] It is clear that the catalytic activity for CO oxidation of the Pt/ZnO prepared by MOF route is twice as high as the activity of the Pt/ZnO obtained by conventional methods. The good catalytic activities of the Pt/ZnO samples may result from metal (Pt)–support (ZnO) interaction and depend on Pt particle size.[12]

In summary, we have for the first time employed MOFs as a precursor to prepare Pt-supporting ZnO nanoparticles based on the intrinsic metal oxide subunits and pores in MOFs, which exhibits excellent catalytic activities for CO oxidation. The present finding provides us a new example of application of the rapidly growing MOF family. The structural diversity of MOFs will show high potential for synthesizing functional materials.

We are grateful to AIST and Kobe University for the financial support. B. Liu thanks MEXT for a Japanese Government Scholarship.

Reference

1 a) T. Uemura, S. Horike, K. Kitagawa, M. Mizuno, K. Endo, S. Bracco, A. Comotti, P. Sozzani, M. Nagaoka, S. Kitagawa, *J. Am. Chem. Soc.* **2008**, *130*, 6781. b) F. Schröder, D. Esken, M. Cokoja, M. W. E. van den Berg, O. I. Lebedev, G. V. Tendeloo, B. Walaszek, G. Buntkowsky, H.-H. Limbach, B. Chaudret, R. A. Fischer, *J. Am. Chem. Soc.* **2008**, *130*, 6119. c) S. Takamizawa, T. Akatsuka, T. Ueda, *Angew. Chem., Int. Ed.* **2008**, *47*, 1689. d) W. Lin, *MRS Bull.* **2007**, *32*, 544. e) R.-Q. Zou, H. Sakurai, S. Han, R.-Q. Zhong, Q. Xu, *J. Am. Chem. Soc.* **2007**, *129*, 8402. f) R.-Q. Zou, H. Sakurai, Q. Xu, *Angew. Chem., Int. Ed.* **2006**, *45*, 2542. g) L. Pan, M. B. Sander, X. Huang, J. Li, M. Smith, E. Bittner, B. Bockrath, J. K. Johnson, *J. Am. Chem. Soc.* **2004**, *126*, 1308. h) H. Li, M. Eddaoudi, M. O'Keeffe, O. M. Yaghi, *Nature* **1999**, *402*, 276.

2 B. Liu, H. Shioyama, T. Akita, Q. Xu, *J. Am. Chem. Soc.* **2008**, *130*, 5390.

3 a) A. Fukuoka, J.-I. Kimura, T. Oshio, Y. Sakamoto, M. Ichikawa, *J. Am. Chem. Soc.* **2007**, *129*, 10120. b) Z. Zhong, J. Lin, S.-P. Teh, J. Teo, F. M. Dautzenberg, *Adv. Funct. Mater.* **2007**, *17*, 1402. c) O. Pozdnyakova, D. Teschner, A. Wootsch, J. Kröhnert, B. Steinhauer, H. Sauer, L. Toth, F. C. Jentoft, A. Knop-Gericke, Z. Paál, R. Schlögl, *J. Catal.* **2006**, *237*, 1. d) O. Pozdnyakova, D. Teschner, A. Wootsch, J. Kröhnert, B. Steinhauer, H. Sauer, L. Toth, F. C. Jentoft, A. Knop-Gericke, Z. Paál, R. Schlögl, *J. Catal.* **2006**, *237*, 17. e) O. S. Alexeev, S. Y. Chin, M. H. Engelhard, L. Ortiz-Soto, M. D. Amiridis, *J. Phys. Chem. B* **2005**, *109*, 23430. f) M. Haruta, *Nature* **2005**, *437*, 1098. g) T. Hayashi, K. Tanaka, M. Haruta, *J. Catal.* **1998**, *178*, 566.

4 D. R. Palo, R. A. Dagle, J. D. Holladay, *Chem. Rev.* **2007**, *107*, 3992.

5 A. J. Esswein, D. G. Nocera, *Chem. Rev.* **2007**, *107*, 4022.

6 J. Gonzalez, R. N. Devi, D. P. Tunstall, P. A. Cox, P. Wright, *Microporous Mesoporous Mater.* **2005**, *84*, 97.

7 a) S. Musić, A. Šarić, S. Popović, *J. Alloys Compd.* **2008**, *448*, 277. b) M. Andrés-Vergés, C. J. Serna, *J. Mater. Sci. Lett.* **1988**, *7*, 970.

8 P. Yang, H. Yan, S. Mao, R. Russo, J. Johnson, R. Saykally, N. Morris, J. Pham, R. He, H. Choi, *Adv. Funct. Mater.* **2002**, *12*, 323.

9 a) A. Bourane, D. Bianchi, *J. Catal.* **2002**, *209*, 114. b) A. Bourane, D. Bianchi, *J. Catal.* **2002**, *209*, 126. c) T. Engel, G. Ertl, *Adv. Catal.* **1979**, *28*, 1.

10 S. Li, G. Liu, H. Lian, M. Jia, G. Zhao, D. Jiang, W. Zhang, *Catal. Commun.* **2008**, *9*, 1045.

11 a) H. Bonnemann, G. A. Braun, *Angew. Chem., Int. Ed. Engl.* **1996**, *35*, 1992. b) J. J. F. Scholten, A. P. Pijpers, A. M. L. Hustings, *Catal. Rev.-Sci. Eng.* **1985**, *27*, 151.

12 a) Z. Xu, F.-S. Xiao, S. K. Purnell, O. Alexeev, S. Kawi, S. E. Deutsch, B. C. Gates, *Nature* **1994**, *372*, 346. b) G. N. Vayssilov, B. C. Gates, N. Rösch, *Angew. Chem., Int. Ed.* **2003**, *42*, 1391.